Si-MFI Crystallization Using a "Dimer" and "Trimer" of TPA Studied with Small-Angle X-ray Scattering

Peter-Paul E. A. de Moor,* Theo P. M. Beelen, and Rutger A. van Santen

Eindhoven University of Technology, Schuit Institute of Catalysis, P.O. Box 513, 5600 MB Eindhoven, The Netherlands

Larry W. Beck and Mark E. Davis

California Institute of Technology, Pasadena, California 91125

Received: February 18, 2000; In Final Form: May 18, 2000

The formation and consumption of precursors and the crystallization of Si-MFI using bis(tripropylammonium) hexamethylene dihydroxide ("dimer" of tetrapropylammonium cation, TPA) and bis(tripropylammonium-*N*-*N*′-hexamethylene)-*N*″,*N*″-dipropylammonium trihydroxide ("trimer" of TPA) as structure-directing agents have been investigated in situ using simultaneous, time-resolved, SAXS and WAXS and using USAXS. The formation of 2.8-nm-sized primary units is observed upon dissolution of the silica source, which is in agreement with results from earlier studies on systems with the TPA cation as a structure-directing agent. Aggregation of these nanometer-scale primary units to 10−15-nm-sized particles is found to be an essential step in nucleation of the zeolite. Crystal growth occurs via the addition of the primary units to the growing crystal. Although the size of the primary units for MFI is independent of the structure-directing agent used, the organic species does have a pronounced influence on the crystal growth step and, therefore, on the crystal growth rate, size, and morphology. The results presented here confirm a common mechanism proposed for organic-mediated crystallization of high-silica zeolites.

Introduction

The elucidation of the mechanisms by which complicated macroscale objects self-assemble remains one of the most difficult challenges. There is a continuing need to understand the rules governing the formation of such complicated structures, which are often of a hybrid organic−inorganic nature (e.g., bone and diatoms). It is crucial to be aware that the assembly processes need not be the same over all length and time scales.

The assembly of pure-silica zeolites by the use of organic molecules that assist in the synthesis process and are accommodated in the final structures is an example of an assembling hybrid system. There are no strong chemical bonds formed between the organic and inorganic fractions of the composite material; the cooperative behavior of weak interactions, e.g., van der Waals forces, dictates the assembly process. Thus, the isolation of intermediates in the process is most likely destructive, and only in situ observations are reliable.

When an organic−zeolite composite is synthesized, organization on length scales from subnanometer to microns is important. At short length scales, information on the ordering of atoms can be obtained. The precursors in the crystallization process are typically in the nanometer range, whereas the product crystals can grow until the micrometer range. To probe the complete broad range of length scales involved in the assembly process, we used a combination of small- and wide-angle scattering of X-rays (SAXS and WAXS, respectively). With the appropriate combination of setups, we are able to probe length scales from interatomic distances up to microns (ultra-small-angle X-ray scattering, USAXS). The use of X-rays allows us to perform in situ experiments on the solutions under hydrothermal conditions, and the high-brilliance synchrotron radiation allows a time resolution shorter than the time scale of the transformation under investigation.

In a previous study on the synthesis of Si-MFI using the TPA cation as a structure-directing agent, we showed a correlation the formation and consumption of nanometer scale precursors to the crystallization mechanism.[1] The formation of nanometer-scale primary units (2.8 nm) was found upon dissolution of the silica source. Aggregation of these particles to ∼10-nm-sized particles was found, depending on the alkalinity of the synthesis mixture (in terms of Si/OH ratio). By tuning the alkalinity, we were able to prepare a synthesis mixture that had only the 2.8-nm-sized primary units and no aggregates. This synthesis mixture was not able to form viable nuclei, but a normal growth of added Si-TPA-MFI seed crystals was found. This illustrates that the aggregation of the primary units is an essential step in the nucleation process, but that these particles do not play a crucial role in the growth process.

To test whether the primary units observed in the zeolite synthesis mixture are specific for the zeolite topology formed, the syntheses of several other zeolite topologies have been investigated. Using one organic structure-directing agent, trimethylene-bis(*N*-benzyl,*N*-methylpiperidinium), both Si-BEA and Si-MTW were prepared.[2,3] The scattering from the heterogeneous gel phase formed under hydrothermal conditions showed strong scattering, but still a difference in the primary units for the two zeolite topologies could be observed. Also,

* Corresponding author. Current address: Exxon Chemical Belgium, Meerhout Polymers Plant, Biezenhoed 2, B-2450 Meerhout, Belgium. Fax: +32 14 867072.

10.1021/jp0006476 CCC: $19.00
Published on Web 07/22/2000

for the crystallization of the structure-type SOD zeolite, a specific size of primary units was observed.[4]

It is well-known that MFI can be prepared with various organic molecules as structure-directing agents. We showed that primary units with the same size were present for systems with four different structure-directing agents.[4] In this reference, we proposed a general mechanism for organic-mediated zeolite crystallization, which involves the formation of nanometer-scale primary units that are specific for the zeolite topology and an aggregation of these primary units to have the formation of viable nuclei. Crystal growth can occur via the addition of primary units.

In this study, we investigate the formation of precursors in the crystallization of Si-MFI from clear solutions using as the structure-directing agent bis(tripropylammonium) hexamethylene dihydroxide and bis(tripropylammonium-*N*-*N*′-hexamethylene)-*N*′′,*N*′′-dipropylammonium trihydroxide.[5] These molecules conceptually are the "dimer" and "trimer" of tetrapropylammonium. The formation of precursors and crystalline product has been investigated in situ using time-resolved, combined SAXS/WAXS and USAXS. The evolution of particle populations in the solution is compared with that of the systems using TPA as a structure-directing agent, and the roles of the different precursors and the structure-directing agent in the crystallization mechanism are discussed.

Experimental Section

Zeolite Synthesis. The recipe and preparation of the synthesis mixtures are based on those of our previous study[1] using TPA as a structure-directing agent, where the chemical composition of the synthesis mixture was [x Na_2O]:[1.22 $(TPA)_2O$]:[10 SiO_2]:[117 H_2O]. In this study, x was varied to obtain Si/OH ratios between 2.12 and 2.72. For the syntheses using bis(tripropylammonium) hexamethylene dihydroxide ("dimer" of TPA) and bis(tripropylammonium-*N*-*N*′-hexamethylene)-*N*′′,*N*′′-dipropylammonium trihydroxide ("trimer" of TPA), the ratio of R/SiO_2 was maintained at 1.22:10 and 0.81:10, respectively, to keep the ratio N^+/SiO_2 constant at 2.44.

The synthesis mixture was prepared by dissolving NaOH (Merck, p.a.) in the structure-directing agent solution. The amount of water was adjusted by addition of distilled water or evaporation by boiling, keeping in mind that the silica source contains some water. The silicic acid (Baker, 10.2 wt % H_2O) was applied through a fine sieve (to avoid lumps of silica in the solution) while the solution was stirred with a magnetic stirrer. Thereafter, the homogeneous dispersion was boiled with stirring for approximately 10 min to obtain a clear solution. The solution was cooled to room temperature in a water bath, corrected for loss of water during boiling, and filtered through a paper filter (Schleicher and Schüll, Schwarzband) and subsequently through a 0.45-μm filter (Schleicher and Schüll, Spartan 30/B). The reaction mixtures were completely clear to the eye and aged for less than 1 h at room temperature before they were heated to the reaction temperature, unless specified otherwise. The reaction temperature was always 125 °C.

Sample Cell. To perform in situ experiments, an electrically heated brass holder containing a rotating round sample cell (Figure 1) was designed. Rotation was necessary to keep the synthesis mixture homogeneous, as only a small spot near the center of the cell was exposed to the X-ray beam. A rate of approximately 2 revolutions per minute appeared to be fast enough to prevent silicalite crystals from precipitating prematurely.

Two clear mica sheets (Attwater and Sons) were used as windows, with spacing provided by a Teflon ring (thickness, 0.5 mm). The liquid sample could be heated hydrothermally up to 175 °C, and contact between the sample and the brass cell was avoided at any moment during the sample preparation and the synthesis. Heating of the sample holder from room temperature to a reaction temperature of 125 °C took only 2 min. This rotating cell was used for both the combined SAXS/WAXS and the USAXS investigations.

In principle, the mica windows of the sample cell could be suspected to be nucleating surface for the silicalite crystals. Many of our experiments have also been performed in Teflon-lined stainless steel autoclaves, and a significant difference in crystallization behavior has never been observed (see, e.g., ref 5). Therefore, we believe that, if any nucleation occurs at the mica surface, this effect does not influence the crystallization process of the bulk to significant extent.

SAXS and USAXS. The combined SAXS and WAXS experiments were performed at station 8.2 of the Synchrotron Radiation Source at Daresbury Laboratory (Warrington, U.K.),[6] using camera lengths of 0.8 m ($0.4 < Q < 7$ nm^{-1}) and 3.4 m ($0.1 < Q < 2.5$ nm^{-1}). With the high-intensity synchrotron radiation and position-sensitive detectors, we were able to collect SAXS and WAXS patterns simultaneously with a good signal-to-noise ratio every two minutes. The data were normalized for the intensity of the X-ray beam and corrected for detector sensitivity prior to background correction. The scattering from water at the reaction temperature was used as a background pattern. For the calibration of the SAXS and WAXS patterns, respectively, the scattering of an oriented specimen of wet rat-tail collagen and the diffraction of a fully crystallized sample of zeolite NaA were used. The wavelength for station 8.2 is fixed at 1.54 Å.

The USAXS experiments were performed at the high-brilliance beamline ID2/BL4 of the European Synchrotron Radiation Facility in Grenoble (Grenoble, France) using a Bonse−Hart type of camera[7] ($0.001 < Q < 0.3$ nm^{-1}). A configuration with two analyzer crystals was used, so no desmearing was necessary. The first analyzer crystal [Si(220)] was used to scan the angle, and there were three reflections in the horizontal plane. A second analyzer crystal [Si(111), two reflections] was used as a collimator in the vertical direction in order to obtain a comparable angular resolution in both the vertical and the horizontal directions. The wavelength of the X-rays was 1.0 Å. A NaI scintillator was used as the detector, which shows a linear response over 4 decades of intensity. Several scans (4−5), over different 2Θ ranges with sufficient overlap, were recorded using different degrees of attenuation of the incident X-ray beam, so that the intensities on the detector were in the linear range. Because of the high brilliance of the undulator beamline ID2, a complete pattern could be recorded in only 15 min, despite the inherent low efficiency of the Bonse−Hart setup and the scanning mode of recording.

SAXS Data Analysis. SAXS data provide information about the presence of different particle populations and about some of their properties, such as particle size distribution, shape, and type of interactions. The size distribution of the (growing) crystals in the synthesis mixtures was determined by fitting the calculated scattering pattern of a population of interacting spheres to the measured curve. In the calculation of the form factor, the crystals were assumed to have a normal size distribution and a spherical shape.[8,9] For calculating the structure factor, the Percus−Yevick approximation for hard-sphere interactions was applied. The influence of the polydispersity on the structure factor was taken into account using the "local monodisperse approximation" of Pedersen,[10] which proves to

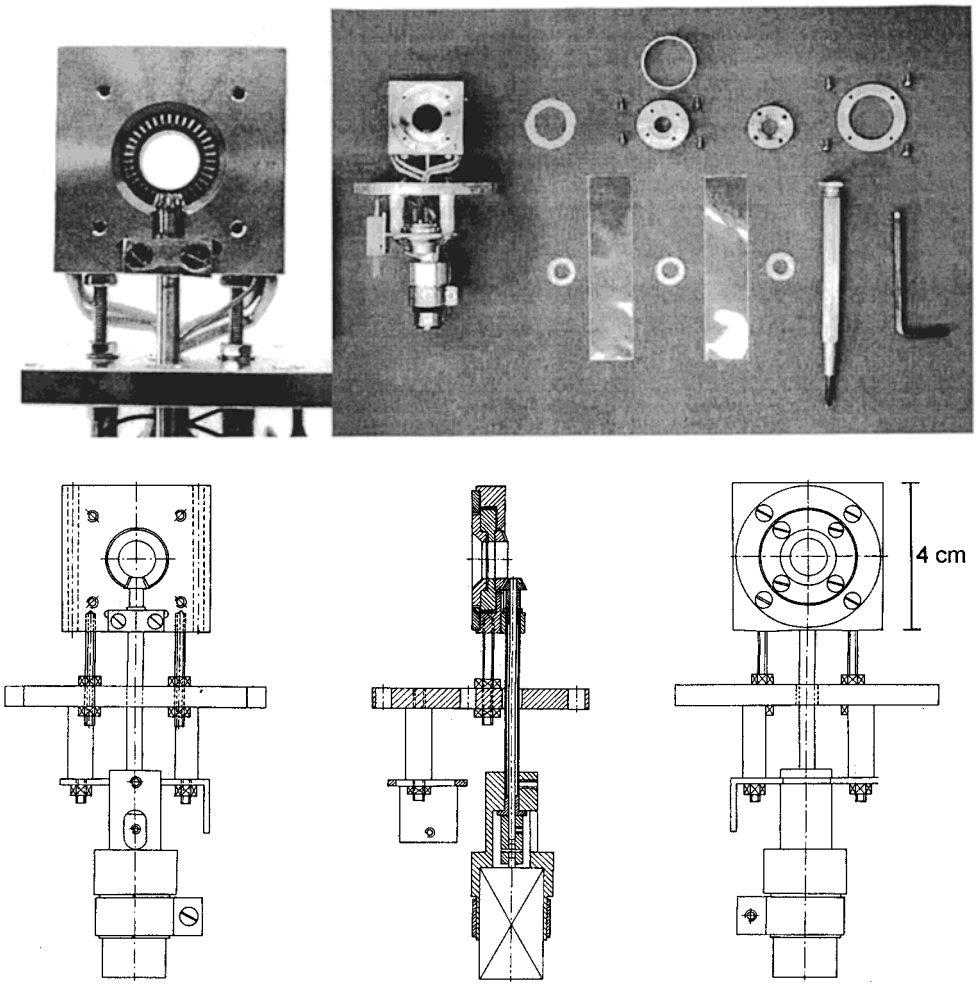

Figure 1. Rotating, electrically heated sample cell used for all scattering experiments. Top left: Close-up of the rotation gear. Top right: All parts of the sample cell. Bottom: Schematic drawing.

give good results up to volume fractions of 0.4. In our experiments, the volume fraction of crystals in the mother liquor was typically 0.05 at full crystallization. The small contribution of the structure factor to the calculated intensity was included for completeness.

The basic data correction, the analysis of the time-resolved data, and the interactive fitting of a calculated scattering pattern to measured data were performed using an in-house-developed GUI-based program called Analyze, written in the IDL programming language.

Results

TPA. The crystallization of Si-MFI from clear water synthesis mixtures with TPA as a structure-directing agent, studied with small-angle X-ray scattering techniques has been reported extensively by us in previous publications.[1,8,11−13] The most relevant results for comparison with the current study are published in ref 1.

Dimer of TPA. Crystallization of Si-MFI using the dimer of TPA as the structure-directing agent was performed from a series of synthesis mixtures having different alkalinities, expressed as the ratio Si/OH. Figure 2 shows clearly that the crystallization behavior is practically independent of the Si/OH ratio, except for the synthesis with the highest alkalinity (Si/OH = 2.12) for which the conversion to crystalline material is much slower. For this synthesis mixture with Si/OH = 2.12, almost no conversion to crystalline material is observed on the time-scale that is needed for the synthesis mixtures with lower alkalinities to complete the sigmoidal crystallization curve (300−400 min).

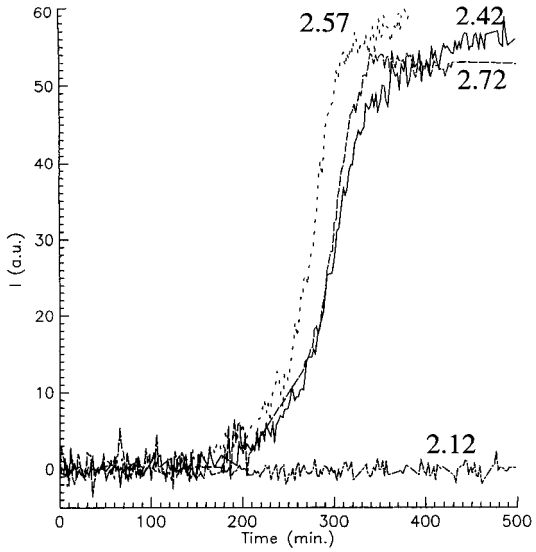

Figure 2. Crystallization behavior for Si-MFI synthesis using the dimer of TPA as the structure-directing agent as determined from the area of the Bragg reflections between 2Θ values of 7.4° and 9.3°. The Si/OH ratios of the synthesis mixtures are denoted at the curves.

The small-angle scattering patterns of the X-rays during the course of the reaction are shown in Figure 3. These plots provide

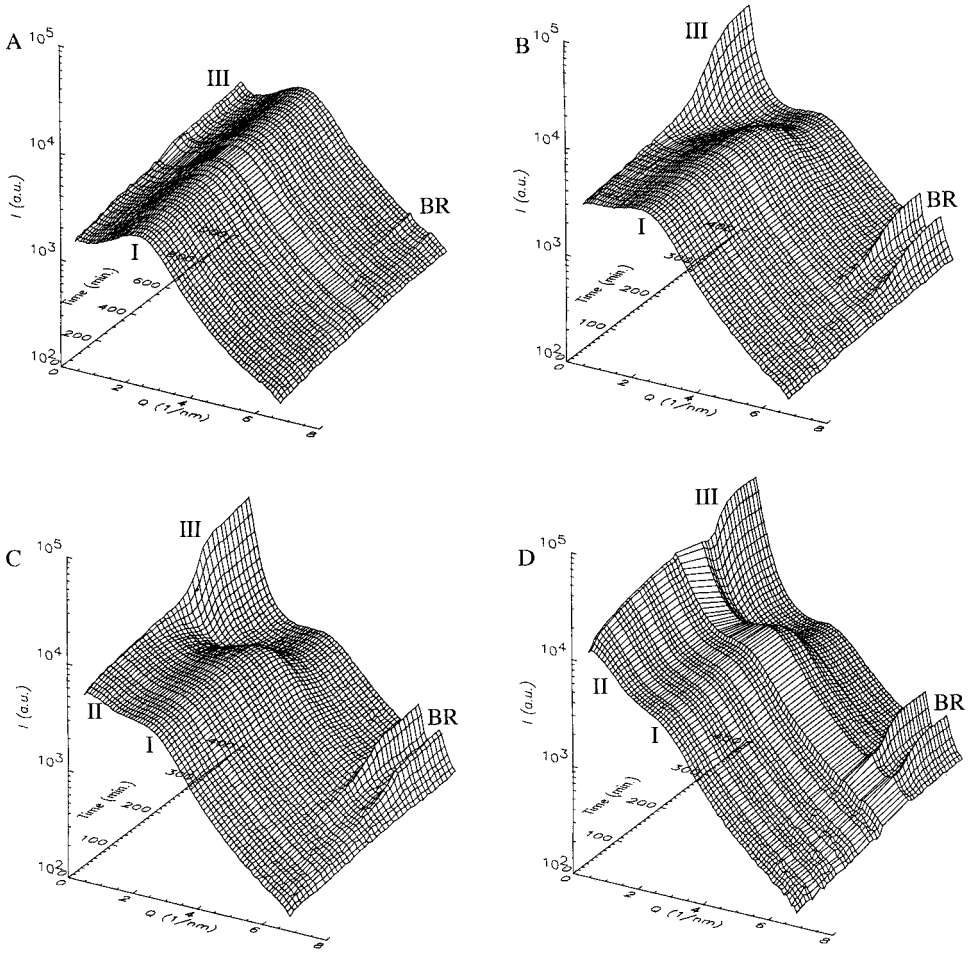

Figure 3. Time-resolved SAXS patterns for Si-MFI crystallization using the dimer of TPA for different Si/OH ratios: (A) 2.12, (B) 2.42, (C) 2.57, and (D) 2.72. Scattering particle types: I = primary units, II = aggregates, III = crystals, and BR = Bragg reflections.

an overview of the particle populations formed and consumed during the whole crystallization process. The maximum observed around $Q \approx 2.2$ in Figure 3A corresponds to primary particles with a size of approximately 2.8 nm. Precursors with the same size have also been observed in the crystallization of Si-MFI with TPA as a structure-directing agent.[1] The presence of these particles is less clear when the alkalinity of the synthesis mixtures decreases (in Figure 3, A → B → C → D). This is due to the presence of a second population of precursor particles with a size of 10−15 nm giving rise to a shoulder in the scattering curve at Q values of 0.5−1.0 nm^{-1}. The number of such particles in the synthesis mixture increases with decreasing alkalinity. With increasing reaction times (going from the front to the back in the plots in Figure 3), the consumption of the two types of precursors is observed. At the same time, two indications of the formation of crystals is observed: the appearance of Bragg reflections at relatively high angles (small length scales) and the increasing scattering intensity due to scattering at the surface of the growing crystals at low angles (large length scales).

The features in the scattering curves due to scattering at the different particle populations are clear in Figure 4, which shows the patterns at various stages during the crystallization process. From the single maximum in Figure 4A, it is clear that only one type of precursor particle is present during the crystallization from the synthesis mixture with the higher alkalinity. The formation of crystalline material is slow, but after 1000 min of heating, small peaks due to Bragg reflections are clearly present in the scattering pattern (Figure 4A′).

The scattering pattern for the synthesis mixture with Si/OH = 2.72 clearly shows the presence of two types of precursor particles prior to the onset of the formation of long-range order (Figure 4D). In addition to the 2.8-nm-sized primary particles observed in all synthesis mixtures, larger (10−15 nm) particles are present. These larger particles are believed to be aggregates of the primary units and will be referred to as aggregates from now on.

The slope of the log I vs log Q representation of the scattering data from the crystals provides information about the morphology of the particles. For smooth spherical particles with a homogeneous density, a slope of −4 is to be expected. The observed slope is significantly different, with a value of approximately −2.8 (see linear fit in panels B, C, and D of Figure 4).

To obtain a more clear overview about whether and how the presence of the different particle types correlate, the scattering intensity at the corresponding angles was plotted as a function of the heating time (Figure 5). The scattering intensity at a certain angle is a measure of the concentration of the scattering entities with the corresponding size in the sample ($d = 2\pi/Q$). The primary particles are present from the onset of the reaction. During the extent of the reaction, but prior to the onset of the formation of the crystals as determined from the area of the Bragg reflections, the aggregates are being formed. Only for the crystallization with the highest alkalinity (Si/OH = 2.12, Figures 4A and 5A) can no scattering at the aggregates be observed. All plots show that the primary particles and the aggregates both are consumed in the crystallization process and,

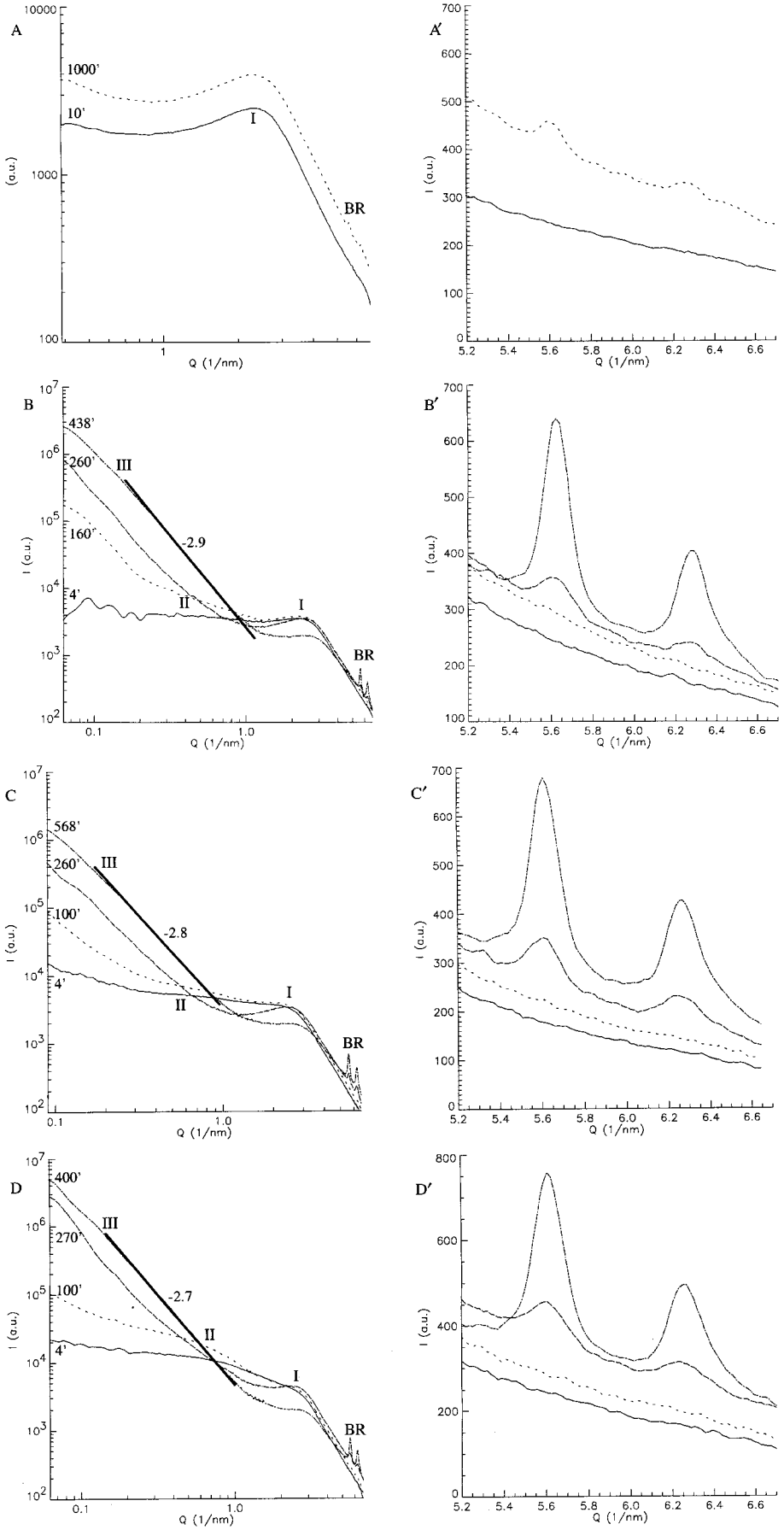

Figure 4. (A−D) SAXS patterns for the synthesis of Si-MFI using the dimer of TPA as the structure-directing agent at various reaction times, as denoted at the curves. In panels B, C, and D the slope of the linear fit to the scattering curve is also provided. (A′−D′) Scattering intensity at the position of the first Bragg reflections for reaction times corresponding to the SAXS curves in A−D. Si/OH ratios of the synthesis mixtures: (A, A′) 2.12, (B, B′) 2.42, (C, C′) 2.57, and (D, D′) 2.72. Scattering particle types: I = primary units, II = aggregates, III = crystals, and BR = Bragg reflections.

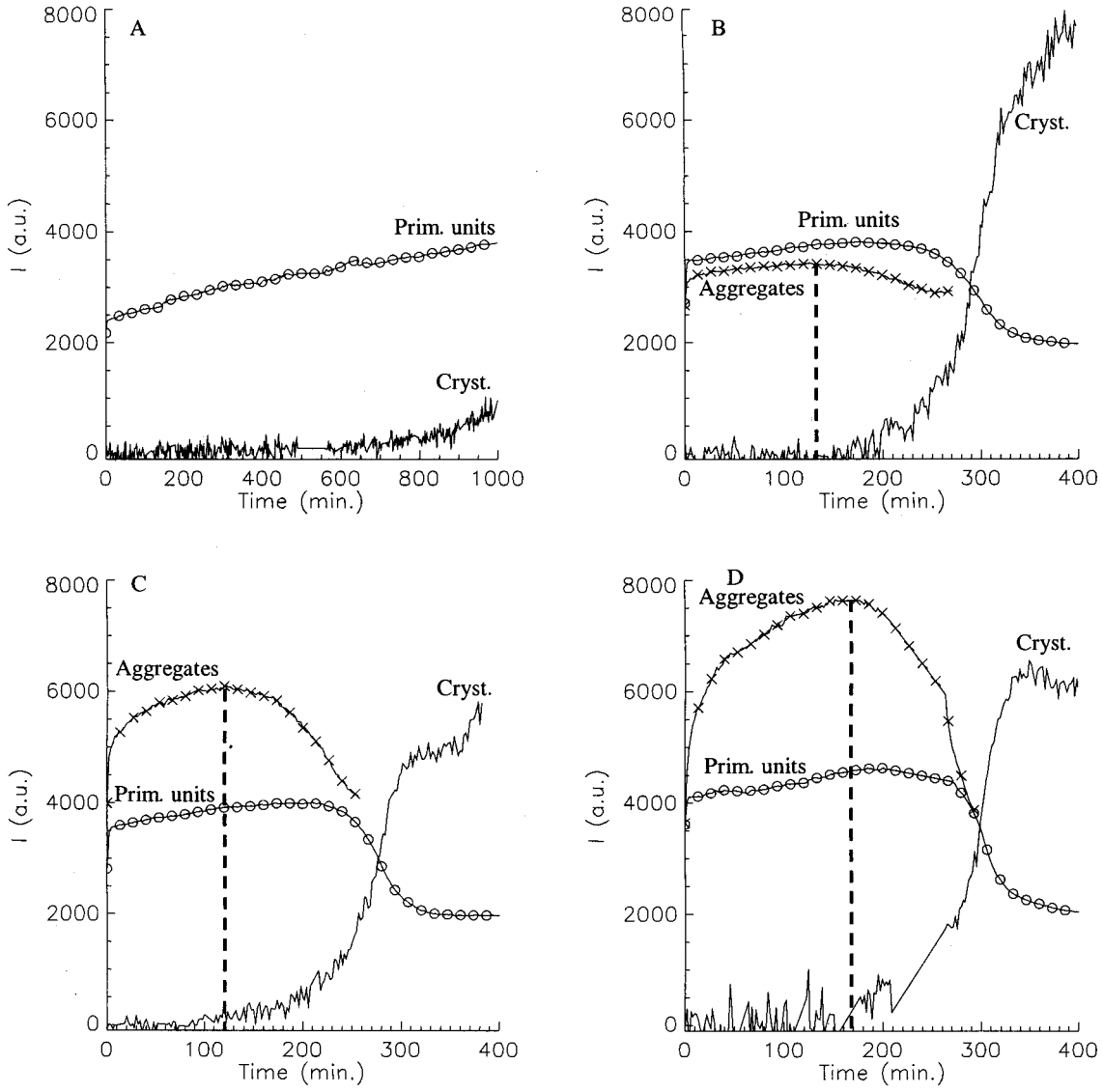

Figure 5. Scattering at the different particle populations for the synthesis of Si-MFI using the dimer of TPA as the structure-directing agent: − = crystallinity, ○ = primary units, and × = aggregates. Si/OH ratios: (A) 2.12, (B) 2.42, (C) 2.57, and (D) 2.72. The dotted vertical lines in panels B, C, and D correspond to the start of the decrease in the concentration of aggregates of primary units.

therefore, can be called precursors in the crystallization process. Although the aggregates appear to be formed in a later stage of the reaction than the primary units, their consumption in the crystallization process starts before that of the 2.8-nm primary units (see vertical dotted lines in panels B, C, D of Figure 5).

Aged Synthesis Mixture with Dimer of TPA. The influence of aging the synthesis mixtures at room temperature prior to heating them to reaction temperature on the formation of precursors and crystals was investigated by comparing a sample that had aged for 9 days with a fresh (aging less than 30 min) synthesis mixture with the same composition, namely, Si/OH = 2.42. The crystallization behavior obtained from the areas of the Bragg reflections shows a more rapid conversion of the synthesis mixture to crystalline material for the aged sample compared to the fresh sample (Figure 6).

The scattering patterns for the fresh (Figure 3B) and aged samples (Figure 7) show the same features during the crystallization process. When the individual scattering curves are compared at various stages in the crystallization process, the characteristics in the patterns for the aged sample (Figure 8) in general resemble those observed for the nonaged synthesis mixture (Figure 4B and B′). However, for the short time of

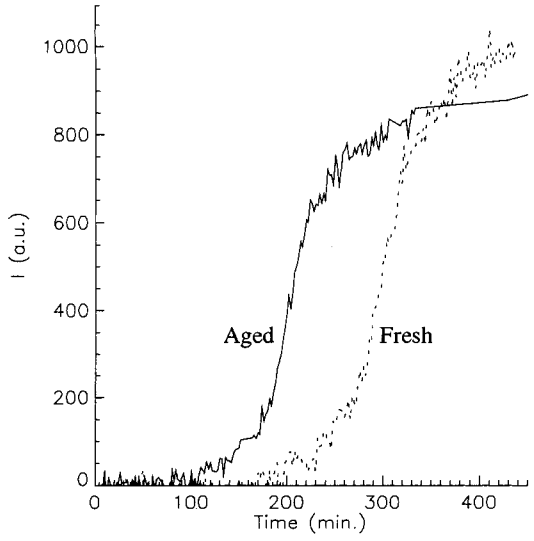

Figure 6. Crystallization behavior for MFI using the dimer of TPA as the structure-directing agent with Si/OH = 2.42 for a fresh synthesis mixture (dotted line) and a synthesis mixture aged at room temperature for 9 days (solid line).

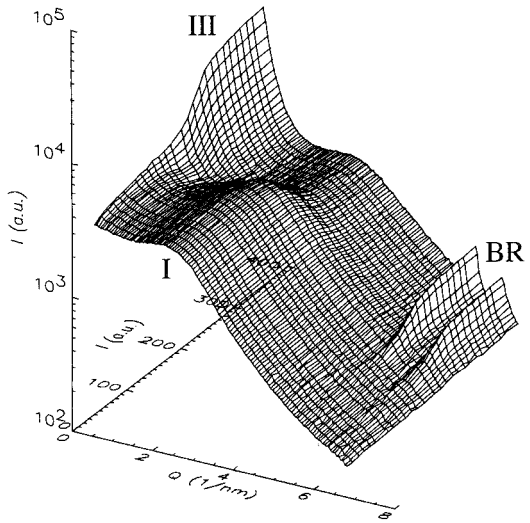

Figure 7. SAXS pattern for Si-MFI crystallization using the dimer of TPA as the structure-directing agent from a synthesis mixture with Si/OH = 2.42 that was aged at room temperature for 9 days prior to being heated to a reaction temperature of 125 °C. Scattering particle types: I = primary units, III = crystals, and BR = Bragg reflections.

heating of 4 min, in the scattering pattern for the aged synthesis mixture, a hump is observed at low scattering angles that is absent in the scattering pattern for the nonaged synthesis mixture. Although the intensity of this hump is not great, it suggests the presence of particles with diameters larger than 30 nm.

The time dependence of the scattering intensity at the different particle populations in the synthesis mixture shows the same trend for the aged sample (Figure 9) compared to the fresh one (Figure 5B). There are, however, two significant differences: First, the reaction times at which the formation and consumption processes of the precursors take place for the aged sample are shorter than those for the nonaged sample. This is in agreement with the faster crystallization process (Figure 6). Second, the scattering intensity at the aggregates is greater for the aged sample than the fresh one, whereas the intensity due to scattering at the primary units is essentially the same for the two samples.

Trimer of TPA. The crystallization of Si-MFI was also performed using a trimer of TPA. The Si/OH ratio was 2.42, and the reaction temperature was 125 °C, as it was also for all other synthesis results presented in this article. Figure 10A shows that the crystallization rate for Si-MFI is slower when the trimer of TPA is used as a structure-directing agent compared to when TPA or its dimer are used. All three crystallization curves show the often-observed sigmoidal trend. However, the final intensity of the Bragg reflections decreases in the order TPA > dimer > trimer. Here, the intensity is the area of the Bragg reflections and, therefore, a measure of the amount of crystalline material in the sample irrespective of the peak broadening due to differences in crystallite sizes. Because the concentration of silica was the same for the three syntheses, this points to differences in conversion of amorphous silica to zeolite MFI. Unfortunately, no other data on the conversion is available for comparison.

Figure 10B also shows that the shape of the Bragg reflections at the end of the crystallization is different for the three templates. The width of the peaks increases in the order TPA < dimer < trimer (e.g., see the peak at $Q = 5.63$ nm^{-1}). For the crystals synthesized using TPA as a structure-directing agent, clearly two separate Bragg reflections are observed at $Q = 6.26$ nm^{-1} and 6.45 nm^{-1} ($2\Theta = 8.80°$ and 9.07°, respectively). However, for crystals prepared using the dimer and trimer, the two peaks cannot be discerned.

The evolution of the small-angle X-ray scattering curves during crystallization from a synthesis mixture with the trimer (Figure 11) shows the same trend as that for the dimer (Figure 3B). On close observation, however, the scattering of the aggregates is stronger for the synthesis with the trimer (Figure 12) compared to that with the dimer (Figure 5B). These figures also show that the scattering intensity from the primary units is independent of the structure-directing agent used.

Using a Bonse−Hart type of camera, smaller scattering angles can be probed that are very difficult to probe with a conventional small-angle X-ray scattering camera. Combining the results obtained with both cameras, information over a very broad range of length scales is available. Using the scattering at very low angles, the changes in the size of the crystals can be followed. At length scales longer than the size of the crystals, information about their organization in the synthesis mixture can be obtained.

Figure 13 shows the combined USAXS and SAXS data for the crystallization of Si-MFI using the trimer of TPA as the structure-directing agent. Now, the whole scattering curve from the crystal particles can be observed. For reaction times less than or equal to 636 min, the scattering pattern levels off to a constant intensity with decreasing scattering angle. This suggests that the crystal particles move free from each other in the synthesis mixture. From a fit of the calculated scattering pattern of a polydisperse system of particles to the experimental curve, information can be obtained on the size of the crystal particles. For reaction times longer than 636 min, a sudden increase in scattering intensity is observed for low angles ($Q < 0.05$ nm^{-1}). This scattering pattern agrees with the aggregation of the crystal particles. Also, a slope of −1.7 is observed in the log I vs log Q plot in the appropriate region.

From the above-mentioned fitting procedure, information can be obtained about the size of the crystal particles in the synthesis mixture (for a detailed description of the fitting procedure, see ref 8). Figure 14 shows that the growth rate is strongly dependent on the structure-directing agent used. The crystal particle growth appears to be linear with time, and the results of a linear fit to the data in the time range of crystal particle growth is given in Table 1. The final size of the crystal particles for the synthesis using the trimer as the structure-directing agent was 70 nm. Although not shown in Figure 14, one can see this also in Figure 13 in which there is no change in the scattering from the individual crystal particles between 636 and 1588 min of reaction.

Discussion

The time-dependent small-angle X-ray scattering data provide information about the formation and consumption of particles in the synthesis mixture during the course of the crystallization process. Below, we will first provide an overview of the different particle populations observed, after which we will elucidate on their role during the crystallization process.

Particle Populations. The scattering patterns for the Si-MFI synthesis mixtures with the dimer or trimer of TPA as structure-directing agents show the presence of four particle types in the size range of nanometers and larger.

The primary units (indicated by "I" in Figure 4D) are observed from the onset of the reaction and probably are formed during the dissolution of the silicic acid in the alkaline structure-directing agent solution. These particles have a size of approximately 2.8 nm and clearly are consumed in the crystallization process.

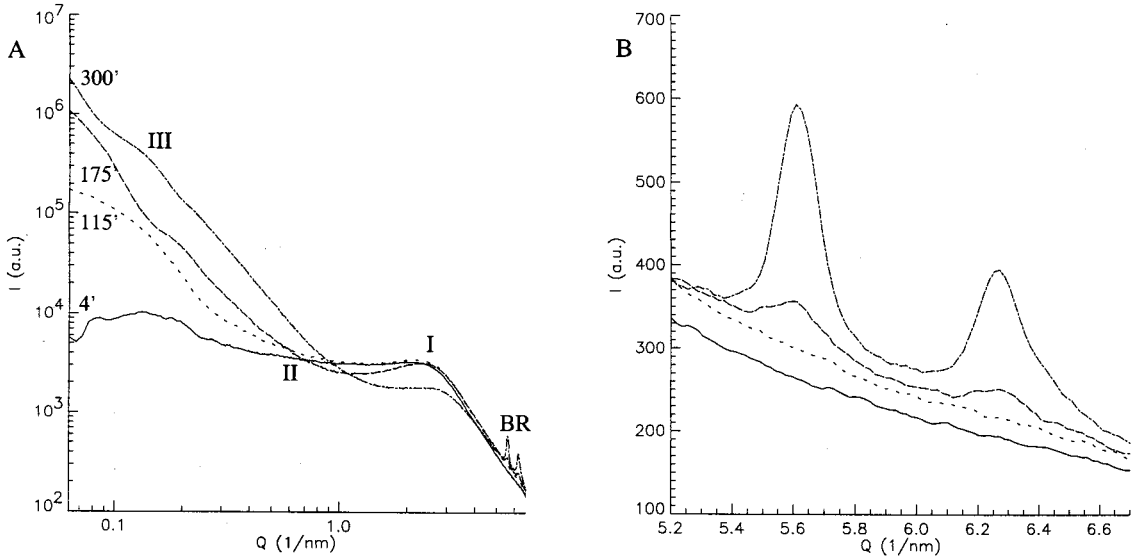

Figure 8. (A) SAXS patterns for the synthesis of Si-MFI using the dimer of TPA as the structure-directing agent at various reaction times, as denoted at the curves. The synthesis mixture was aged for 9 days at room temperature prior to being heated to a reaction temperature of 125 °C. (B) Scattering intensity at the position of the first Bragg reflections for reaction times corresponding to the SAXS curves in panel A.

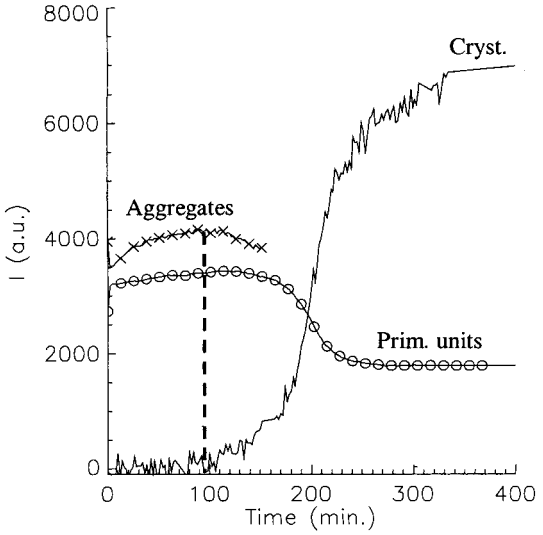

Figure 9. Scattering at the different particle populations for the synthesis of Si-MFI using the dimer of TPA as the structure-directing agent from a synthesis mixture aged for 9 days at room temperature prior to heating: − = crystallinity, ○ = primary units, and × = aggregates. The dotted vertical line corresponds to the start of the decrease in the concentration of aggregates of primary units.

The precursor population (indicated by "II" in Figure 4D) are particles with a size of 10−15 nm that are believed to be aggregates of primary particles. These particles are formed in the synthesis mixture after the formation of the primary units, but before the onset of crystallization, as determined from the observation of Bragg reflections. These so-called aggregates are consumed during the course of the reaction (e.g., see Figure 5D).

The third population of particles are the product Si-MFI crystals, which have a size of up to several hundred nanometers in these experiments. There are two methods for tracking the formation of the crystals in our data: from the scattering at the crystal surface, observed at relatively large length scales (small angles, see "III" in Figure 4D), and from the diffraction at the internal crystalline lattice of the crystals (Bragg reflections, indicated by "BR" in Figure 4D).

During the crystal growth process, the individual Si-MFI crystals behave as discrete particles in the solution, as evident from the constant scattering intensity for length scales larger than the size of the individual particles. At the end of the growth process, the individual crystals form aggregates (fourth particle population) with a size larger than 6 μm (see region "IV" in Figure 13).

As one would expect in a self-assembly process in which macroscopic structures are formed from microscopic particles, the observed particles become larger as the reaction time increases.

Primary Units. The primary units observed here in the systems with the dimer and trimer of TPA show a strong similarity to those observed in the system with the TPA cation reported earlier.[1] The same size of 2.8 nm was observed for all systems resulting in the Si-MFI topology. The nanometer-sized particles were present in the synthesis mixture from the onset of the reaction for all three structure-directing agents. Moreover, the particles were consumed at the same stage during the crystallization process. Therefore, we believe that the primary units observed in the systems with the dimer and trimer of TPA are similar to those observed in systems studied in the presence of TPA.

The primary units formed in the presence of TPA have been thoroughly investigated. NMR experiments showed that silicate species interact with the TPA cations prior to the formation of long-range order.[14] TPA is clearly identified as being present in the precursor particles from contrast-variation SANS experiments on synthesis mixtures[15] and Raman experiments on particles extracted from aqueous solution.[16] Ordering in the silica (observation of 560 cm^{-1} IR band) in structures typical for the MFI crystal topology was observed before the onset of the crystallization.[17] On the basis of NMR experiments on extracted particles formed during the dissolution of silica in the presence of high concentrations of the TPA cation, a model was presented for the structure of the primary units.[18] This model envisions the primary units as a 1.3 × 4.0 × 4.0 slab containing 9 TPA cations[19] in which the MFI structure is already fully developed.

Using several assumptions, we can make an estimate of the concentration of the primary particles in the solution. First, we assume that any silica identified as being present in polymeric species is part of the primary particles. An average value of

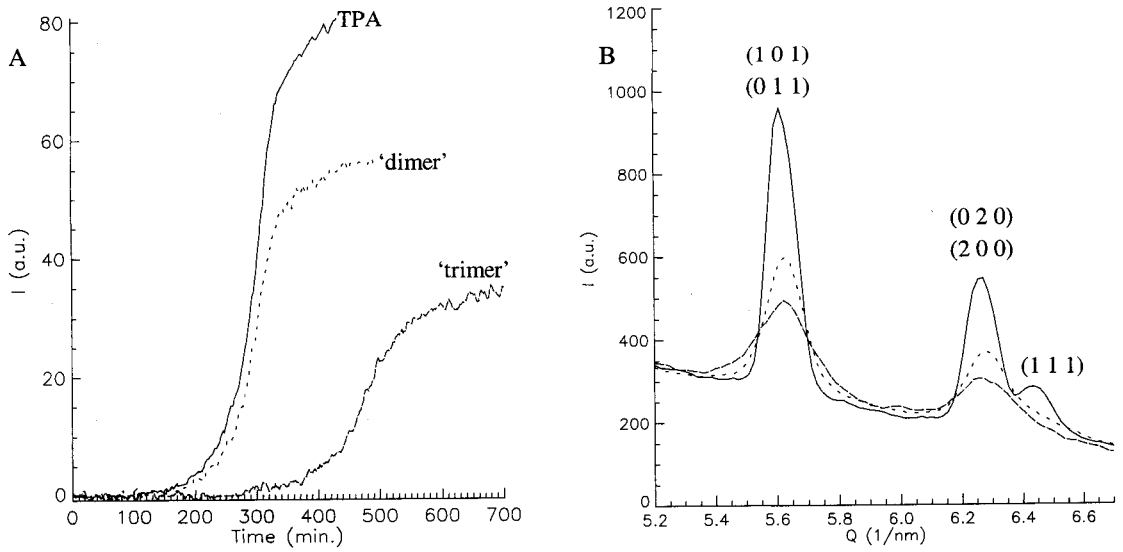

Figure 10. Crystallization behavior as determined from the area of the Bragg reflections between 2Θ values of 7.4° and 9.3° for Si-MFI synthesis using TPA, the dimer of TPA, or the trimer of TPA as the structure-directing agent. The Si/OH ratio is 2.42 for all synthesis, and the crystallization temperature is 125 °C.

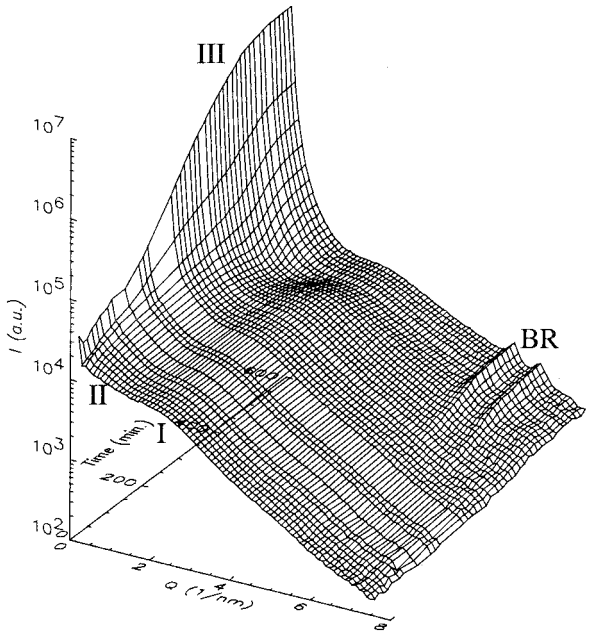

Figure 11. SAXS pattern for Si-MFI crystallization using the trimer of TPA as the structure-directing agent. Scattering particle types: I = primary units, II = aggregates, III = crystals, and BR = Bragg reflections.

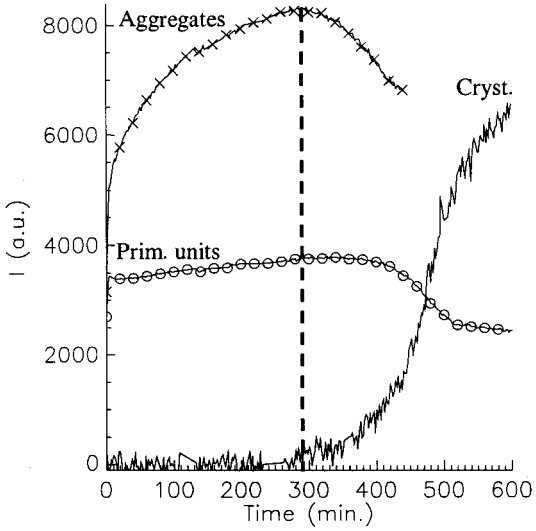

Figure 12. Scattering at the different particle populations for the synthesis of Si-MFI using the trimer of TPA as the structure-directing agent: − = crystallinity, ○ = primary units, and × = aggregates. The dotted vertical line corresponds to the start of the decrease in the concentration of aggregates of primary units.

0.9 is used from the results and references by Schoeman.[20] The structure of the primary particles is believed to be MFI-like, so the density and composition (with TPA) of Si-TPA-MFI is used. This results in concentrations on the order of 9×10^{18} and 5×10^{18} primary units per mL, assuming shapes of a sphere with a diameter of 2.8 nm and a $1.3 \times 4.0 \times 4.0$ slab, respectively.

In a recent publication, we showed that the presence of the primary units can be extended to the crystallization of other zeolites than MFI. The crystallization of all-silica zeolite beta and MTW from a synthesis gel contain trimethylene-bis(*N*-benzyl,*N*-methylpiperidinium) was investigated.[3] Although the same structure-directing agent and similar synthesis mixtures were used for the formation of the different zeolites, a difference was observed in the primary units.

It is well-known that the zeolite Si-MFI can be prepared with several structure-directing agents. In another paper, we showed that the primary units formed are the same for synthesis mixtures with four different structure-directing agents (TPA, dimer of TPA, trimer of TPA, and trimethylene-bis(*N*-hexyl,*N*-methylpiperidinium).[4] Moreover, different silica sources have been used (TEOS and silicic acid), and the preparation methods and consistencies of the synthesis mixtures were different (clear liquid and gel). The results presented in Figures 2−5 show that some features of the synthesis mixture can drastically change when the alkalinity is varied (e.g., rate of conversion to crystalline material), but the size (2.8 nm) and concentration (from scattering intensity) of the primary units is found to be constant. These results indicate that the observed primary particles are specific for the zeolite topology formed, but that their presence alone is not sufficient for zeolite nucleation.

In principle, information concerning the structure of particles can be derived from SAXS patterns. However, in the cases investigated, several complicating factors make it very difficult to obtain reliable results about the structure of the primary units.

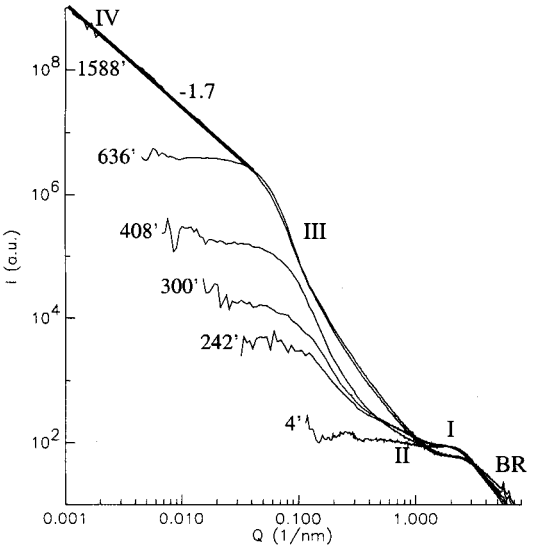

Figure 13. Combined USAXS and SAXS patterns for the synthesis mixture of Si-MFI using the trimer of TPA as the structure-directing agent. Reaction times at 125 °C are denoted at the curves. Scattering particle types: I = primary units, II = aggregates, III = crystals, IV = aggregates of crystals, and BR = Bragg reflections.

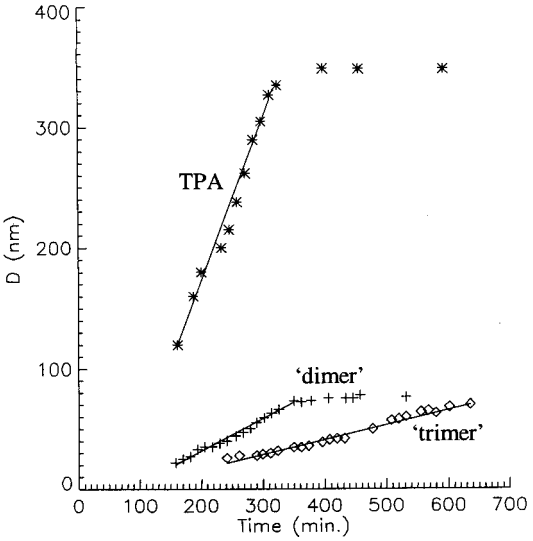

Figure 14. Crystal particle size for the synthesis of Si-MFI using TPA, its dimer, and its trimer as the structure-directing agents with Si/OH = 2.42 at 125 °C. The lines are linear fits to the data in the growth region.

TABLE 1: Crystallization Data for MFI with Different Templates at Si/OH = 2.42 and 125 °C

structure-directing agent	induction (min)	growth rate (nm/min)	final size (nm)
TPA	73	1.35	350
dimer	80	0.27	72
trimer	63	0.12	70

First of all, the concentrations are high, so one has to take into account the interference between the particles. No model accurately describing the interaction between the primary units is available to date (see section Aggregates of Primary Units below). It is also unlikely that all particles in the silicate solution are exactly the same, so the distribution in the morphologies has to be taken into account. This is inherently the case when the system under investigation forms nuclei and growing crystals. Therefore, we believe it is not possible to derive reliable structure information from the SAXS patterns measured in our studies. It may be possible to do the reverse, that is, to test whether a proposed system is in agreement with the measured patterns by calculating the scattering pattern for the theoretical system.

Our only effort in fitting calculated patterns to the experimental curves was for the growing crystals (ref 8). Here, we assumed the crystal population to be a polydisperse system of spheres with a homogeneous density that had hard-sphere interactions. The combination of polydispersity and interacting particles was described using the local monodisperse approximation. This hard-sphere approximation assumes negligible contribution of the surface charge to the particle distribution. This may be true for the crystals, but the chance is small that this assumption holds for the (much smaller) primary particles and their aggregates.

Aggregates of Primary Units. The precursor particles of 10−15 nm in size (aggregates of primary units) are not present in the synthesis mixtures from the onset of the crystallization process, but they are formed during the hydrothermal treatment (see panels B, C, and D of Figure 5).

The concentration of these aggregates appears to depend on the alkalinity of the synthesis mixture, whereas the concentration of the individual primary units was constant. For the synthesis mixture with the highest alkalinity (Si/OH = 2.12), no scattering from the aggregates could be observed. For this system, the conversion to crystalline material was found to be extremely slow (see Figure 2). Similar observations were made for Si-MFI crystallization using TPA as the structure-directing agent.[1] In that case,it was shown that the rate of conversion to crystalline material for different alkalinities is determined by the rate of nucleation and that the rate of crystal growth is independent of the alkalinity in the range studied. For the systems with the dimer of TPA as the structure-directing agent, this is also the case. The slow conversion to crystalline material for the system with Si/OH = 2.12 is due to a low rate of nucleation, which is a result of the low concentration of aggregates of primary units.

The role of the aggregates in the formation of viable nuclei, and therefore the rate of crystallization, is confirmed by a comparison of the aged synthesis mixture with a fresh one. From the scattering intensities, it is clear that the concentration of aggregates during hydrothermal treatment is higher in the aged sample (Figure 9) than in a fresh sample with the same composition (Figure 5B). Figure 6 illustrates that the higher concentration of aggregates correlates with a faster conversion to crystalline material.

To be able to calculate the small-angle scattering patterns for a system of particles that is not infinitely dilute, one needs to account for the particle interactions. The presence of the maximum in the scattering curves at $Q \approx 2.5$ (see Figure 4) indicates that there is a significant influence of the interparticle structure factor on the scattering pattern.[21,22] Schoeman[23] attempted to describe the interactions between the primary units with an extended Derjaguin−Landau and Verwey−Overbeek (DLVO) theory. The results from the model were that the repulsive interactive energy between the negatively charged particles cannot be overcome by their thermal energy. This means that, according to this theory, no formation of aggregates is possible. The results presented here clearly show that aggregation of the 2.8-nm-sized primary units to 10−15-nm aggregates does occur in the synthesis mixtures. The decrease in the concentration, as evident from a decrease in their scattering intensity after the onset of crystallization (Figure 5B, C, and D), shows that the formation of these particles is reversible. The difference between the outcome of the theory and the observations here or in a previous publication[1] illustrates

that the proposed model[23] does not completely describe the interaction between the particles. In a more recent study based on AFM measurements and DLVO simulations including electrostatic repulsion, Nikolakis et al.[24] obtained results that support a mechanism in which the rate-limiting step for growth of silicalite is the addition of the 2.8-nm-sized primary particles, as proposed by us.

Crystal Growth Rate/Role of Template. The crystal growth rate for Si-TPA-MFI was found to be independent of the alkalinity of the synthesis mixture,[1] but the concentration of aggregates of primary units was found to be dependent on the alkalinity. The growth rate of the crystals, therefore, is independent of the concentration of the aggregates, and crystal growth was even observed for systems in which no sign of the aggregates could be found (experiments with seeded Si-TPA-MFI growth in ref 1). Therefore, we are confident that the aggregates of primary units do not play a role in the crystal growth process.

The type of structure-directing agent used in the synthesis mixture shows a distinct influence on the crystal growth rate, as is evident from the crystal size evolution during the hydrothermal treatment measured in situ using USAXS (Figure 14). The crystal growth rate decreases when the size of the organic structure-directing agent increases from TPA to its dimer and its trimer.

Furthermore, it has been observed that the structure-directing agent used has a distinct influence on the morphology of the crystals formed.[5] The particles synthesized in the presence of TPA are more or less spherical, whereas the dimer results in more irregularly shaped particles, and clusters of needle-shaped crystals are obtained using the trimer. The shape of the crystals is reflected in the form factor contribution of the scattering intensity. In the appropriate range in the scattering pattern, this can result in a different slopes in the log I vs log Q representation:[25] a one-dimensional rod will give a slope of -1, a flat sheet will result in a slope of -2, and a homogeneous sphere will give a slope of -4. Here, a slope of approximately -2.8 is observed for the crystals synthesized using the dimer (see Figure 4B, C, and D). Several interpretations of this slope by itself are possible, but it is in agreement with the SEM observations: the individual crystallites have a sheetlike appearance, whereas the overall cluster resembles a ball of crystallites.

The individual crystallites (regions with a certain crystal orientation that can be part of a cluster) are much smaller in the systems synthesized using the dimer and trimer compared to those formed using the TPA cation. This is in agreement with the increase in peak width in the WAXS patterns of the crystals (Figure 10B). For the dimer and trimer, the peaks at $Q = 6.26$ and 6.44 nm^{-1} are not resolved, which can be due to peak broadening and/or to a change in relative intensities due to changes in position of the template in the zeolite pores.

The 2.8-nm-sized primary units discussed before show structural and compositional similarity with the resulting zeolite. Also, their consumption correlates with the formation of crystalline material. Therefore, it is expected that these particles play an important role in both the nucleation (as aggregates) and crystal growth processes. Their appearance, however, seems to be independent of the template used, whereas the crystal growth does depend on the template.

The above results indicate that the template used does not have a major impact on the structure of the nanometer-sized primary units as long as it produces MFI, but it does have a determining role on how these particles connect to the growing crystal. This means that the structure-directing agent used determines the growth rate of the individual crystal faces and, therefore, has a distinct influence on the crystal shape and size.

Crystal Aggregation. As observed before for the synthesis with the TPA cation as the structure-directing agent, the aggregation of the discrete crystals is also observed for the dimer-based (not shown) and trimer-based synthesis (Figure 13, region IV) at the end of the crystallization process. Although this does not provide information on the role of precursors in the crystallization mechanism, it does indicate that there are changes in the synthesis mixture. It is interesting that this process is found for all three structure-directing agents.

The size of these aggregates is larger than 6 μm (the largest length scale probed by USAXS). In electron microscopy images, these aggregates of crystals have never been observed, which indicates that they are vulnerable and do not survive the sample treatment (filtration and drying). The slope of the log I vs log Q representation is -1.7, which corresponds to aggregates with a mass fractal dimension of 1.7 that can be formed by a fast, diffusion-limited aggregation process.[26−28] Such a process results in open, three-dimensional structures. Given the size of the particles forming these structures (the crystals), the pores between the particles must be in the meso- and macro-pore range. In silica chemistry, it is well-known that such structures can become denser and stronger through reorganization of the amorphous silica, which generally results in an increase in the mass fractal dimension. This process is expected to be very slow in our case, because the building blocks are thermodynamically relatively stable crystals. It would be interesting to investigate whether it is possible to strengthen these large aggregates of relatively small crystals so that the resulting structure could withstand drying and handling. In this way, a macroscopic zeolite material could be obtained that showed a combination of macro-, meso-, and micropores.

Conclusions

The formation of 2.8-nm-sized primary units in the synthesis of Si-MFI appears to be independent of the structure-directing agent and of synthesis parameters such as alkalinity, silica source, and temperature. The synthesis of different zeolite types results in a different size of primary units, indicating that the primary units are specific for the zeolite topology formed.

The aggregation of the primary units to 10−15-nm-sized particles is an essential step in the formation of viable nuclei.

The crystal growth probably occurs via the addition of primary units to the growing crystal. The structure-directing agent has a distinct influence on the connection of the growth units to the crystal surface and, therefore, the crystal growth rate, size, and morphology.

These results confirm the existence of a common mechanism in the organic-mediated crystallization of high-silica zeolites.

References and Notes

(1) De Moor, P.-P. E. A.; Beelen, T. P. M.; van Santen, R. A. *J. Phys. Chem. B* **1999**, *103*, 1639−1650.

(2) Tsuji, K.; Davis, M. E. *Microporous Mater.* **1997**, *11*, 53−64.

(3) De Moor, P.-P. E. A.; Beelen, T. P. M.; van Santen, R. A.; Tsuji, K.; Davis, M. E. *Chem. Mater.* **1999**, *11*, 36−43.

(4) De Moor, P.-P. E. A.; Beelen, T. P. M.; Komanschek, B. U.; Beck, L. W.; Davis, M. E.; van Santen, R. A. *Chem. Eur. J.* **1999**, *5*, 2083−2088.

(5) Beck, L. W.; Davis, M. E. *Microporous Mesoporous Mater.* **1998**, *22*, 107−114.

(6) Bras, W.; Derbyshire, G. E.; Ryan, A. J.; Mant, G. R.; Felton, A.; Lewis, R. A.; Hall, C. J.; Greaves, G. N. *Nucl. Instrum. Methods Phys. Res., Sect. A* **1993**, *326*, 587.

(7) Diat, O.; Bösecke, P.; Lambard, J.; De Moor, P.-P. E. A. *J. Appl. Crystallogr.* **1997**, *30*, 862.

(8) De Moor, P.-P. E. A.; Beelen, T. P. M.; Komanschek, B. U.; Diat, O.; van Santen, R. A. *J. Phys. Chem. B* **1997**, *101*, 11077−11086.
(9) Mulato, M.; Chambouleyron, I. *J. Appl. Crystallogr.* **1996**, *29*, 29−36.
(10) Pedersen, J. S. *J. Appl. Crystallogr.* **1994**, *27*, 595−608.
(11) De Moor, P.-P. E. A.; Beelen, T. P. M.; van Santen, R. A. *Microporous Mater.* **1997**, *9*, 117−130.
(12) De Moor, P.-P. E. A.; Beelen, T. P. M.; van Santen, R. A. *J. Appl. Crystallogr.* **1997**, *30*, 675−679.
(13) De Moor, P.-P. E. A.; Beelen, T. P. M.; Komanschek, B. U.; van Santen, R. A. Nanometer Scale Precursors in the Crystallization of Si-TPA-MFI. *Microporous Mesoporous Mater.* **1998**, *21*, 263−269.
(14) Burkett, S. L.; Davis, M. E. *J. Phys. Chem.* **1994**, *98*, 4647−4653.
(15) Watson, J. N.; Iton, L. E.; Keir, R. I.; Thomas, J. C.; Dowling, T. L.; White, J. W. *J. Phys. Chem. B* **1997**, *101*, 10094−10104.
(16) Schoeman, B. J. In *Progress in Zeolite and Microporous Materials*; Chon, H., Ihm, S. K., Uh, Y. S., Eds.; Studies in Surface Science and Catalysis Series; Elsevier Science: New York, 1997; Vol. 105, pp 647−654.
(17) Burkett, S. L.; Davis, M. E. *Chem. Mater.* **1995**, *7*, 920−928.
(18) Ravishankar, R.; Kirschhock, C. E. A.; Knops-Gerrits, P.-P.; Feijen, E. J. P.; Grobet, P. J.; Vanoppen, P.; De Schryver, F. C.; Miehe, G.; Fuess, H.; Schoeman, B. J.; Jacobs, P. A.; Martens, J. A. *J. Phys. Chem. B* **1999**, *103*, 4960−4964.
(19) Kirschhock, C. E. A.; Ravishankar, R.; Verspeurt, F.; Grobet, P. J.; Jacobs, P. A.; Martens, J. A. *J. Phys. Chem. B* **1999**, *103*, 4965−4971.
(20) Schoeman, B. J. *Microporous Mater.* **1997**, *9*, 267−271.
(21) Porod, *G. Monatsh. Chem.* **1972**, *103*, 395−405.
(22) Kratky, O.; Porod, G. Z. *Phys. Chem., Neue Folge* **1956**, *7*, 236−241.
(23) Schoeman, B. J. *Miroporous Mesoporous Mater.* **1998**, *22*, 9−22.
(24) Nikolakis, V.; Kokkoli, E.; Tirrell, M.; Tsapatsis, M.; Vlachos, D. G. *Chem. Mater.* **2000**, *12*, 845−853.
(25) Pedersen, J. S. *Adv. Colloid Interface Sci.* **1997**, *70*, 171−210.
(26) Schmidt, P. W. In *The Fractal Approach to Heterogeneous Chemistry*; Avnir, D., Ed.; John Wiley and Sons: New York, 1989; pp 67−79.
(27) Meakin, P. In *On Growth and Form: Fractal and Nonfractal Patterns in Physics;* NATO-ASI Series; Martinus Nijhoff Publishers: Dordrecht, The Netherlands, 1986; Vol. 100, pp 111−135.
(28) Teixeira, J. In *On Growth and Form: Fractal and Nonfractal Patterns in Physics*; NATO-ASI Series; Martinus Nijhoff Publishers: Dordrecht, Germany, 1986; Vol. 100, pp 145−162.